T · H · E
OHIO STATE UNIVERSITY

Final Report on Electromagnetic Scattered Field Evaluation and Data Compression using Imaging Techniques

I. J. Gupta and W. D. Burnside

The Ohio State University

ElectroScience Laboratory

Department of Electrical Engineering
Columbus, Ohio   43212

50272-101

REPORT DOCUMENTATION PAGE	1. REPORT NO.	2.	3. Recipient's Accession No.

4. Title and Subtitle	5. Report Date
Final Report on Electromagnetic Scattered Field Evaluation	September 1996
and Data Compression using Imaging Techniques	6.

7. Author(s)	8. Performing Org. Rept. No.
I. J. Gupta and W. D. Burnside	727625-2

9. Performing Organization Name and Address	10. Project/Task/Work Unit No.
The Ohio State University	
ElectroScience Laboratory	11. Contract(C) or Grant(G) No.
1320 Kinnear Road	(C)
Columbus, OH 43212	(G) NAG3-1496

12. Sponsoring Organization Name and Address	13. Report Type/Period Covered
National Aeronautics and Space Administration	Final Report
21000 Brookpark Rd.	14.
Cleveland, Ohio 44135	

15. Supplementary Notes

16. Abstract (Limit: 200 words)

This is the final report on Project #727625 between The Ohio State University and NASA, Lewis Research Center, Cleveland, Ohio. Under this project, a data compression technique for scattered field data of electrically large targets is developed. The technique was applied to the scattered fields of two targets of interest. The backscattered fields of the scale models of these targets were measured in a compact range. For one of the targets, the backscattered fields were also calculated using XPATCH computer code. Using the technique all scattered field data sets were compressed successfully. A compression ratio of the order 40 was achieved. In this report, the technique is described briefly and some sample results are included.

17. Document Analysis   a. Descriptors
    DATA COMPRESSION
    SCATTERED FIELDS
    HIGH FREQUENCY

b. Identifiers/Open-Ended Terms

c. COSATI Field/Group

18. Availability Statement	19. Security Class (This Report)	21. No. of Pages
	Unclassified	34
	20. Security Class (This Page)	22. Price
	Unclassified	

(See ANSI-Z39.18)   *See Instructions on Reverse*   OPTIONAL FORM 272 (4-77)
Department of Commerce

Contents

List of Figures

Chapter 1

Introduction

The scattered fields associated with an electrically large target vary rapidly with frequency and aspect angle. To accurately obtain the scattered fields of the target at all frequencies and aspect angles of interest, therefore, vast amounts of scattered field data must be collected and stored. For example, for a 25' long target to avoid aliasing error the scattered field data should be collected every 10 MHz and 0.05° angular increment. In this case, one has to store 1601×7201 complex numbers to cover 2-18 GHz frequency band for a single azimuthal cut and one polarization. One can easily estimate the amount of data needed to be stored for multiple azimuthal cuts and full polarization. In this situation, one will be interested in a technique which can be used to compress the scattered field data. Under this project, a data compression technique for scattered field data of electrically large targets is developed. In this report, a brief description of the technique is given. The technique was applied to the scattered fields of two targets of interest. The backscattered fields of the scale models of these targets were measured in a compact range. For one of the targets, the backscattered fields were also calculated using XPATCH computer code [1]. Using the technique all scattered field data sets were successfully compressed. A compression ratio of the order of 40 was achieved. Some sample results are also included in this report. Though the technique is described for inverse synthetic aperture radar (ISAR) data associated with the backscattered fields of a target, the technique can be applied to SAR or ISAR data associated with monostatic or bistatic scattered fields of a target.

It is well known that the scattered fields of an electrically large target exhibit a highly localized behavior which is related to the target's scattering mechanisms. The response associated with an individual scattering mechanism does not vary rapidly with frequency and/or aspect angle. The rapid variations in the total scattered fields of an electrically large target are due to the relative phase difference between the individual scattering mechanisms. Thus, one can achieve data compression by separating and then storing the responses associated with individual scattering mechanisms of a target. Initially we developed [2] a scattered field data compression technique based on this concept. This technique, however, mainly focussed on radar targets which are dominated by line-of-sight scattering mechanisms that can be isolated easily in a radar image of the target. The scattering mechanisms associated with a real world target usually have very sophisticated phase histories and exhibit non-linear frequency and aspect dependence. Under this contract we focused on developing a scattered field data compression technique for these realistic scattering mechanisms.

The data compression technique developed under this project uses the focused radar image of a target to estimate the locations of various scattering mechanisms associated with the target. The individual scattering mechanisms, instead of being viewed as isolated scattering centers, are classified into two groups — complex point scattering mechanisms and line segment scattering mechanisms. The locations of the centers of these mechanisms are obtained from the radar image. Next, using the location information, the response associated with individual scattering mechanisms is extracted from the total scattered fields. The location information and properly sampled response associated with individual scattering mechanisms are stored as a compressed data set. To reconstruct the total scattered fields from the compressed data set, the individual scattering mechanism responses are combined after proper phase adjustment. Note that the reconstructed data may not be exactly the same as the original data. To reduce the reconstruction error, one may have to store an extremely large number of scattering mechanisms, which is not desired. Thus, there is a tradeoff between the compression ratio and the reconstruction error. In the technique, a threshold level is set in the image domain so that the scattering

2

mechanisms whose image magnitude is greater than the threshold level are extracted and stored. As expected, the lower the threshold, the smaller the reconstruction error, and the smaller the compression ratio. The technique presented here, therefore, is a lossy compression process. It is designed so that the highest compression ratio and the smallest reconstruction error can be obtained.

The rest of the report is organized as follows. In Chapter 2, the ISAR images of a real world target are presented. It is shown that the ISAR images depend on the frequency band and aspect angle region of the scattered field data used to generate the radar image. From these images some guidelines for frequency bands and aspect angle regions to be used for data compression are established. These radar images are also used to define the complex point and line segment scattering mechanisms. In Chapter 3, the procedure used to identify the line segment mechanisms and the complex point mechanisms in a radar image is given. The procedure used to extract and store the response of individual scattering mechanism is also discussed in this section. A description of the scattered field data reconstruction procedure from the compressed data set is also given in this chapter. Chapter 4 contains some sample results. Finally, Chapter 5 contains a summary and some general conclusions of this work.

Chapter 2

Radar Images of a Complex Target

Figure 2.1 shows ISAR images of a complex target (model) at 40°, 60° and 155° aspect angles. The backscattered fields of the target were measured in a compact range over 2–18 GHz frequency band and 0°–240° aspect region using 10 MHz frequency step and 0.1° angular step. The 60° aspect angle represents nose-on incidence for this target. The radar images are obtained by using the scattered field data over 6–12 GHz frequency band and ±15° aspect angle region. The radar images are shown in the radar fixed coordinate system (radar is fixed and the target is rotating). Note that, as expected, the radar image of the target changes with aspect angle. Also, the radar images can be described by a set of points and straight lines. Not only the locations of these points and straight lines but also the number of points and straight lines describing the image vary with aspect angle. Thus, one can not use a single radar image covering the scattered fields over the whole aspect region to find the various scattering mechanisms associated with the target. For this reason, in the technique, radar images at 5° angular increment are used to locate the scattering mechanisms associated with the target. The response of these scattering mechanisms is then used to reconstruct the scattered field data over ±5° about the center aspect angle. Note that the smaller the angular increment between two adjacent radar images, the better will be the reconstructed data. However, it will also lead to a poorer compression ratio. The 5° angular increment, therefore, is a good choice. Also, in the technique, ±15° aspect angle region around the center aspect angle is used to generate the
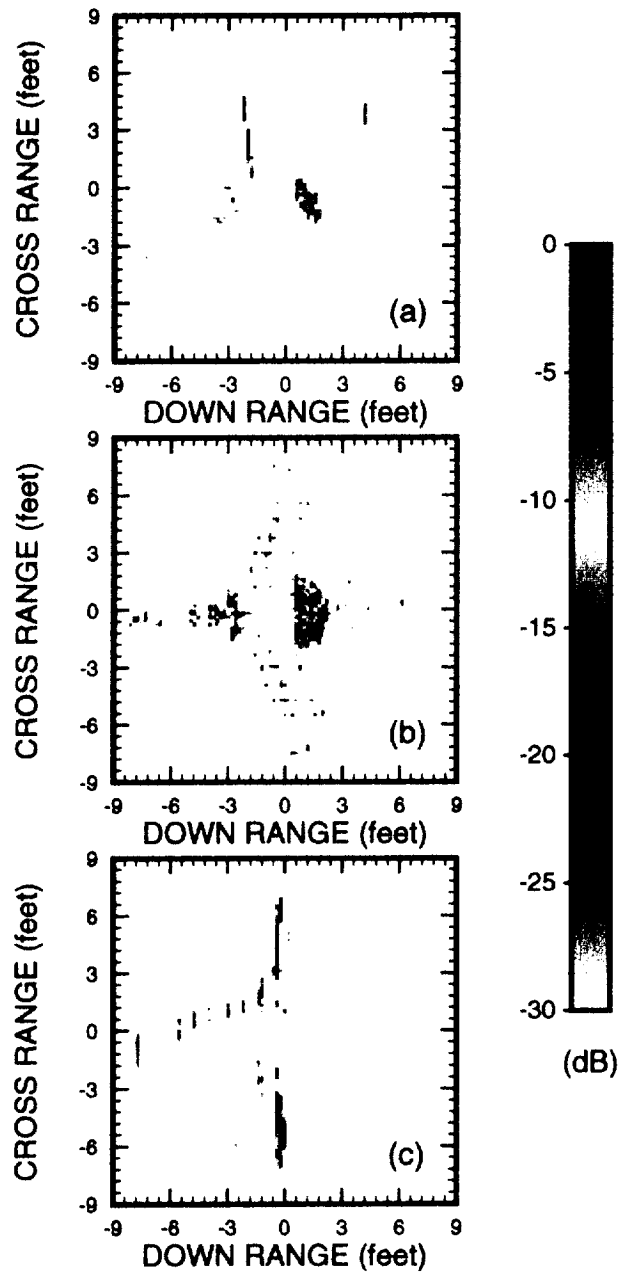
4

Figure 2.1: ISAR images of the complex target at a) 40° center aspect angle, b) 60° center aspect angle, and c) 155° aspect angle. 6–12 GHz frequency band.

radar images of the target. This choice leads to approximately the same cross range resolution as the down range resolution.

Figure 2.2 shows ISAR images of the complex target at 30° aspect angle when the scattered field data over different frequency bands are used to generate the radar images. All other parameters are the same in all the radar images. Again scattered field data over ±15° aspect region around 30° central aspect angle are used in the radar image. Note that the radar image of the target changes with the frequency band used to generate the radar image. Some of the scattering mechanisms present at the lower frequency band (2–6 GHZ) disappear for the higher frequency bands (6–12 GHz and 12–18 GHz). Therefore, one can not use a single radar image covering the scattered fields over the whole frequency band (2–18 GHz) to find the various scattering mechanisms associated with the target. For this reason, in this study, radar images over three independent frequency bands are used to locate the scattering mechanisms. The three frequency bands are 2–6 GHz, 6–12 GHz and 12–18 GHz. One could have selected the frequency bands to be 2–4 GHz, 4–8 GHz and 8–18 GHz; however for the target under consideration, the first set provided smaller reconstruction errors. Again, by using more frequency bands, one may be able to reduce the reconstruction error. However, this will also lead to a poorer compression ratio. Thus, there is a tradeoff between the number of frequency bands and the reconstruction error.

From the above discussion, it is clear that the scattering mechanisms associated with a real world target are highly dependent on the aspect angle and frequency. For the sake of data compression, however, the important consideration is that the scattering mechanisms are focused in the image domain so that their individual responses can be extracted and compressed. From the radar images in Figures 2.1 and 2.2, it is also clear that the various scattering mechanisms focus at a point or along a line segment. Thus, using the image domain behavior, various scattering mechanisms can be classified as a complex point scattering mechanisms or a line segment scattering mechanisms. Note that the term "complex point scattering mechanism" instead of "point scattering mechanism" has been purposely used here. A point scattering mechanism, generally, means an ideal point scattering center. On the other hand, a

6
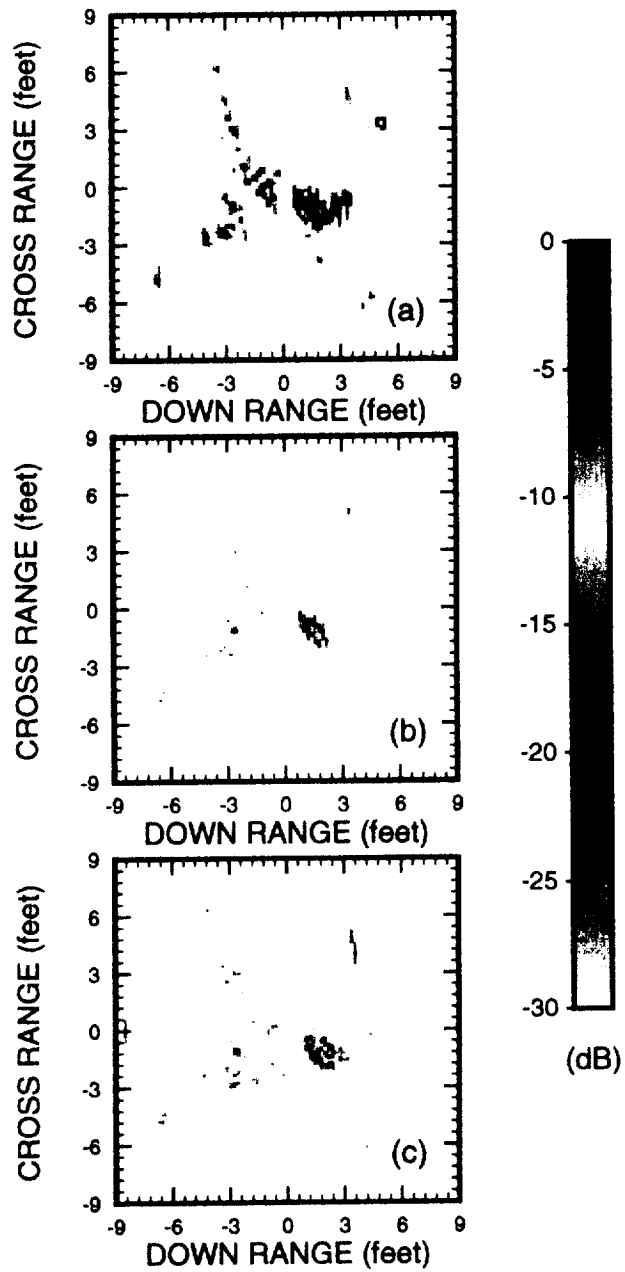
Figure 2.2: ISAR images of the complex target for a) 2–6 GHz frequency band, b) 6–12 GHz frequency band, and c) 12–18 GHz frequency band. Center aspect angle is 30°.

complex point scattering mechanism has aspect and frequency dependent scattered fields but focuses at a point in the image domain. In the next chapter, a brief description of the method used to locate the scattering mechanism in the image domain is described. Also, the methods used to extract and store the two mechanisms are discussed.

Chapter 3

Mechanism Detection, Extraction and Storage

In this chapter, methods used to detect (locate) the various scattering mechanisms associated with a target is described. Also, the methods used to extract and store the scattered fields associated with individual mechanisms are discussed. Finally, the method used to reconstruct scattered fields of the target at the desired frequency and aspect angle is described.

3.1   Mechanism Detection

The first step in the scattered field data compression is the detection (locating) of various scattering mechanisms. As mentioned above, various scattering mechanisms are located in the image domain in the form of complex point scatterers or line segment scatterers. Therefore, first a focussed radar image of the target in radar fixed coordinate system is generated using the scattered field data in the desired frequency band and ±15° aspect region around the desired center aspect angle. Next, the maximum value of the image domain data is determined. Then the line segments and the complex point scatterers whose complex amplitudes are higher than a certain threshold level[1] are located in the radar image. Thus, the data compression technique proposed here is a threshold process.

---

[1]Threshold level is set in the beginning. It was found that a 25 dB level (below the image maximum) is a good choice for complex point scatterers and a 20 dB level is a good choice for line segment scatterers.

Different techniques are used to locate the complex point scatterers and the line segment scatterers. The line segment scatterers are located first. Once a line segment scatterer is located, the image domain response in the neighborhood of the line segment is set to small values before locating the other scatterers. The complex point scatterers are located by searching for a local maxima in the image. A three-point parabolic fit is applied along the down range as well as along the cross range to obtain a better estimate of the local maxima. To reduce the total number of complex point scattering mechanisms, the point scatterers with small separation are combined such that the location of the strongest one is stored. The location of the strongest complex point scattering mechanism is stored first followed by the second strongest point scattering mechanism and so on.

There are many sophisticated line image detection algorithms reported in the literature [3, 4]. Most of them are designed for arbitrarily located line segments. However, since a line segment in a radar image represents the scattered fields from a long straight edge or nearly planar geometry, the incident wave (for backscattering) has to be normal to the straight edge or nearly planar geometry. Therefore, in the radar fixed coordinate system the line segment scattering mechanisms will appear near normal to the down range axis or almost parallel to the cross range axis. Thus, in the technique, the line segment scattering mechanisms are located by searching for line images which are near normal to the down range axis (constant down range distance). Once a line image is detected its length is calculated. If the length is more than the cross range resolution, the line image is assumed to represent a line segment scattering mechanism. Next, the line image is divided into small segments of length equal to the cross range resolution. The centers of these small segments is stored as the locations of the various line segment scattering mechanisms. Note that many (at least two) line segment scattering mechanisms are used to represent a single physical scattering mechanism. The line segment scattering mechanisms are also numbered from the strongest to the weakest. The methods used to extract the response of these two scattering mechanisms are described next.

10

3.2 Mechanism Extraction

One can use a two-dimensional image gating process [2, 5] to extract the response of the individual scattering mechanisms. The gate size will dictate the frequency step size and the aspect angle step size between the independent samples of the extracted data. The smaller the gate, the larger the step sizes. In this study the gate size is selected such that the independent frequency step size is little more than 1 GHz and independent aspect angle step size is little more than 3°. This approach, however, has a couple of problems. First, transforming the image domain data to the frequency-aspect domain from the gated focused radar image involves a lot of computation and thus is not an efficient process. Second, in general, the image domain data is obtained by applying some weights to the original scattered field data in the frequency-aspect domain. After image domain gating, one can not exactly compensate for these weights.

An alternative approach is used in this work. In this approach, a two-dimensional smoothing process [2] is applied to the frequency-aspect domain scattered field data used to generate the corresponding radar image. In the smoothing process, the phase center of the scattered field data is shifted to the location of the scattering mechanisms to be extracted. Next, a weighted averaging (low pass filtering) is applied to the phase adjusted data. The frequency domain averaging is carried out first and then aspect domain averaging is applied. Again, the amount of averaging carried out is such that the frequency step size and aspect size between independent samples is little more than 1 GHz and 3°, respectively. Once the response of the desired scattering mechanism is extracted, it is subtracted from the original scattered field data. The phase center of the subtracted scattered field data is moved to the original phase reference point. This scattered field data is used to extract the responses of the remaining scattering mechanisms. In the data compression technique, the responses of the line segment scattering mechanisms are extracted first followed by the complex point scattering mechanisms. Also, as expected, the stronger scattering mechanisms are extracted first.

11

3.3 Mechanism Storage

Remember the radar images of the target are generated at a 5° aspect increment and the total frequency band (2–18 GHz) is divided into three subbands. Thus, for each image aspect angle, there are three sets of scattering mechanisms. The response of every scattering mechanism in each set is stored at a 1 GHz frequency increment to cover the frequency subband for that set. As mentioned before, for each image aspect angle, the response of each individual scattering mechanism is used to reconstruct scattered field data over $\pm 5°$ aspect region around the image center aspect angle (ϕ_a). To accomplish this, the response of a complex point scattering mechanism is stored at $\phi_a - 3°$, ϕ_a and $\phi_a + 3°$ aspect angles. A three-point Lagrange interpolation is used to obtain the response over $\phi_a \pm 5°$ aspect angle region. The aspect response of a line segment scattering mechanism, as discussed below, is stored a little bit differently.

A line segment scattering mechanism, as discussed earlier, has a long uniform cross-range image. Therefore, its aspect angle response would be a *sinc* function. In the main beam region, a *sinc* function can be approximated by a Gaussian distribution and can be expressed as

$$A(\phi) \;=\; A(\phi_0)\exp\left(-(\phi - \phi_0)^2/2\sigma^2\right) \tag{3.1}$$

where $A(\phi)$ is the magnitude at the desired aspect angle ϕ, ϕ_0 is the aspect angle at which the magnitude is the maximum and σ^2 is the variance of the Gaussian function. Note that one needs ϕ_0, $A(\phi_0)$ and σ^2 to completely define 3.1. Using the magnitude of the extracted response of a line segment mechanism, these three parameters are obtained and stored. One also needs to store the phase information for reconstruction of the scattered field data. The phase of the extracted response of a line segment is stored at $\phi_0 - 0.5°$, ϕ_0 and $\phi_0 + 0.5°$, where ϕ_0 has been defined above. A three-point Lagrange interpolation is used to obtain the phase over $\phi_a \pm 5°$ aspect angle region, where ϕ_a is the image aspect angle.

Note that six real numbers are stored to define the aspect response of a line segment scattering mechanism at a given frequency. For a complex point scattering

mechanism, the aspect response (complex value) at 3 aspect angles is stored. Thus, the total amount of storage is the same for the two mechanisms.

3.4 Data Reconstruction

The scattered field data reconstruction at a given aspect angle ϕ and frequency f is carried out using one of the two different approaches depending on the value of ϕ. If ϕ coincides with one of the image aspect angles (ϕ_a) then a single compressed data set is used for data reconstruction. Let $\phi = \phi_a^i$, where superscript i is used to define the ith image aspect angle, and frequency f is in the jth subband (remember that the total frequency band is divided into three subbands); then, the (i, j) compressed data set is used for data reconstruction. A three-point Lagrange interpolation is used to obtain the response of every complex point scattering mechanism and every line segment scattering mechanism at the desired frequency. The individual scattering mechanism responses are then phase corrected to account for their different locations. The phase corrected responses are summed to obtain the total scattered field data.

When the desired aspect angle does not coincide with any image aspect angle then two compressed data sets are used for data reconstruction. Let $\phi_a^i < \phi < \phi_a^{i+1}$ and f is in the jth frequency subband, then the (i, j)th and $(i + 1, j)$th compressed data sets are used for data reconstruction. The data reconstruction for each compressed data set is carried out independently. The reconstructed scattered field data is then given by

$$E_r(f, \phi) \;=\; \frac{1}{5} \left(\left(\phi_a^{i+1} - \phi \right) \cdot E_r^{i,j} + \left(\phi - \phi_a^i \right) E_r^{i+1,j} \right) \tag{3.2}$$

where $E_r^{i,j}$ is the reconstructed data using the (i, j)th compressed data set. For each scattering mechanism in a given compressed data set, aspect interpolation is carried out before frequency interpolation.

Some sample results are given in the next chapter.

13

Chapter 4

Sample Results

The above mentioned procedure was used to compress and store the scattered field data of the model target from 15° to 225° aspect angle region. The threshold level for the complex point scatterers was set to be -25 dB; whereas the threshold level for the line segment scatterers was set to be -20 dB. From the compressed data, the scattered field data were reconstructed over the whole aspect region and frequency band. Figure 4.1 shows correlation between the original scattered field data and the reconstructed scattered field data versus aspect angle. The frequency domain as well as the time domain correlation is shown in the figure. The correlation is defined as

$$R(\phi) \;\; = \;\; \left| \frac{\int E_0(\phi, k) E_r^*(\phi, k) dk}{\int |E_0(\phi, k)| \; |E_r(\phi, k)| dk} \right| \tag{4.1}$$

where $E_0(\phi, k)$ is the original scattered field data in the frequency or time domain and $E_r(\phi, k)$ is the reconstructed scattered field data in the frequency or time domain. The time domain data was obtained by applying an inverse Fourier transform to the frequency domain data. The frequency domain data was multiplied by Kaiser-Bessel weights before transforming the data to the time domain.

Note that the reconstructed data shows good correlation with the original scattered field data for all aspect angles. In both the frequency and time domains the average correlation for all aspect angles is more than 0.95, which is very good. In certain aspect regions, the correlation is little bit low; however, it is more than 0.85 for all aspect angles, which is still good.

To demonstrate the quality of the compression process, ISAR images of the target are generated using the reconstructed and original scattered field data along critical
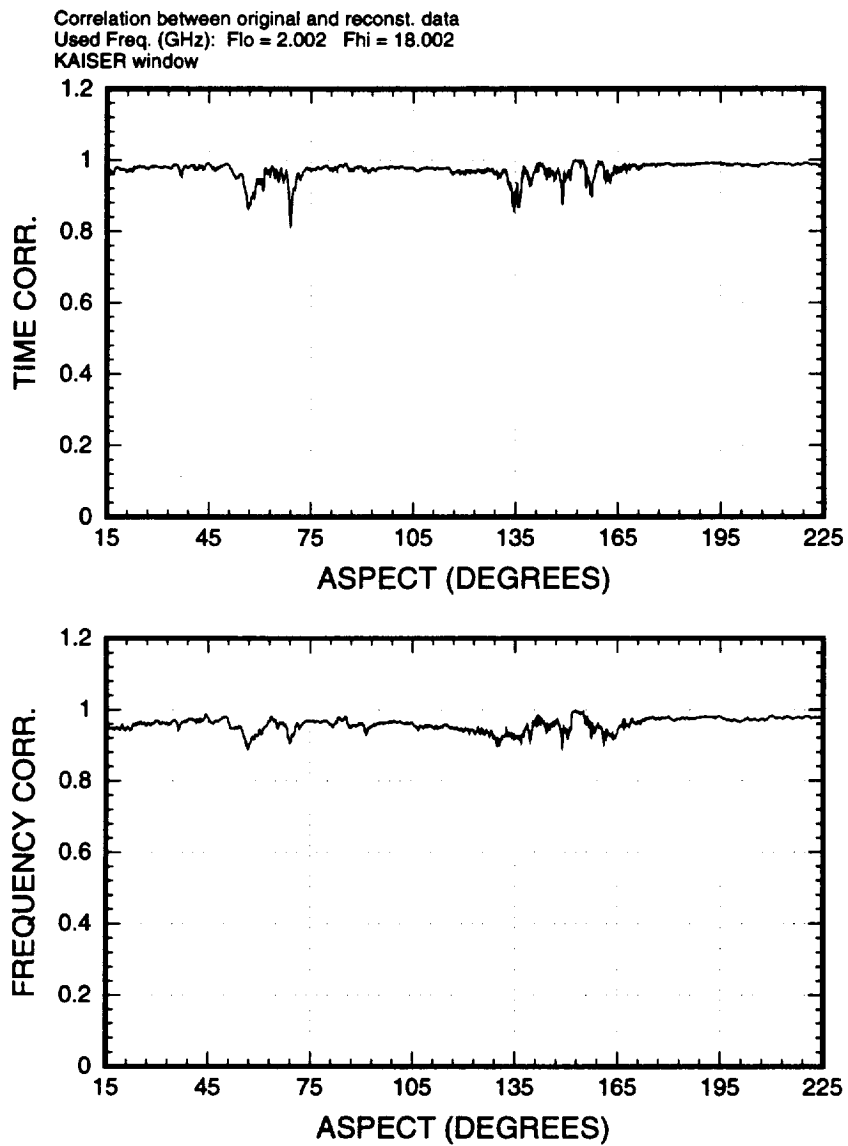
Figure 4.1: Time and frequency domain correlation between the original data and the reconstructed data.

aspect regions. Figures 4.2–4.4 show the ISAR image at 70° aspect angle. Figure 4.2 contains the ISAR image for 2–6 GHz frequency band, Figure 4.3 contains the ISAR images for 6–12 GHz frequency band; whereas, Figure 4.4 contains the ISAR image for 12–18 GHz frequency band. In all the figures, plot (a) is the ISAR image obtained using the original scattered field data; whereas, plot (b) is the ISAR image obtained using the reconstructed scattered field data. Note that the reconstructed scattered field data ISAR images look very similar to the original scattered field data ISAR images.

Figures 4.5-4.7 show the ISAR images when the center aspect angle is 155°. All other parameters are the same as before. Again, one can draw the same conclusions; i.e., the reconstructed scattered field data is a good representation of the original scattered field data.

Table 4.1 shows the total number, the maximum and the minimum number of line segment and complex point scatter mechanisms detected for each frequency band. Based on the detected numbers, the total size of the compressed data set is equal to

$$3 \times (5 \times (395 + 2030) + 7 \times (301 + 1796) + 7 \times (448 + 1890)) = 129,510.$$

The factor 3 accounts for the three aspect angle samples for each image; whereas the factors 5, 7 and 7 are the total number of frequency samples (1 GHz increment) in the three bands. The size of the original scattered field data set is $1601 \times 2101 = 3,363,701$ (10 MHz frequency increment and 0.1° angle increment). This leads to a compression ratio of approximately 26, which is a high compression ratio.

Another interesting observation to be made from the data in Table 4.1 is that the variation between the number of line segment mechanisms detected at different aspect angles is quite high (minimum 0 to maximum 52 in 12–18 GHz frequency band). The same is true for complex point scattering mechanisms. This again stresses the need for generating radar images for many aspect angles and multiple frequency bands. Also, the maximum number of point mechanisms is way too high. One generally does not want to store so many point mechanisms. Figure 4.8 shows the correlation between the original and reconstructed scattered field data when the number of complex point
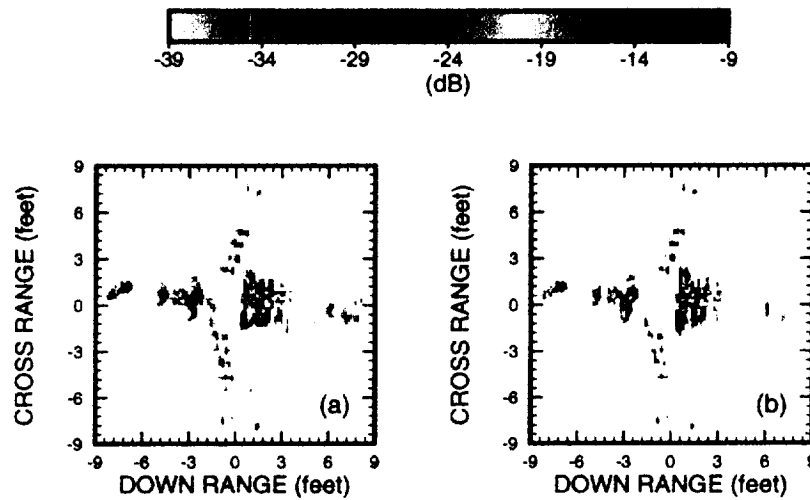
16

Figure 4.2: Original data (a) and reconstructed data (b) ISAR images of the complex target. 2–6 GHz frequency band and 70° center aspect angle.
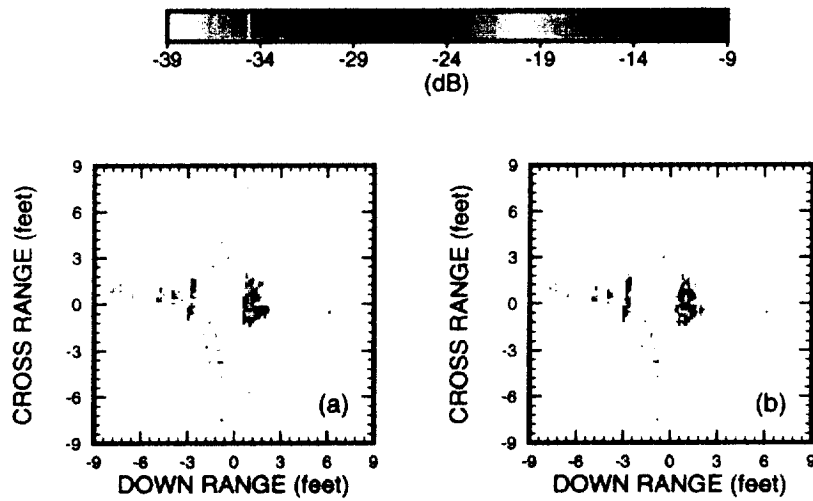

Figure 4.3: Original data (a) and reconstructed data (b) ISAR images of the complex target. 6–12 GHz frequency band and 70° center aspect angle.
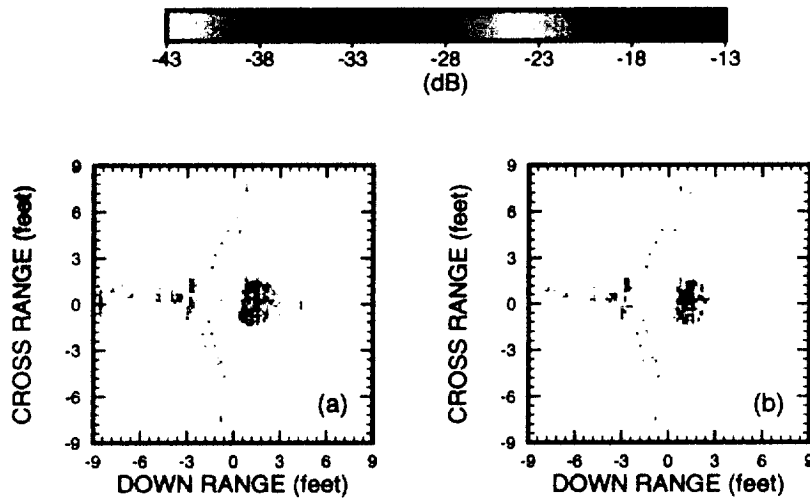
Figure 4.4: Original data (a) and reconstructed data (b) ISAR images of the complex target. 12–18 GHz frequency band and 70° center aspect angle.

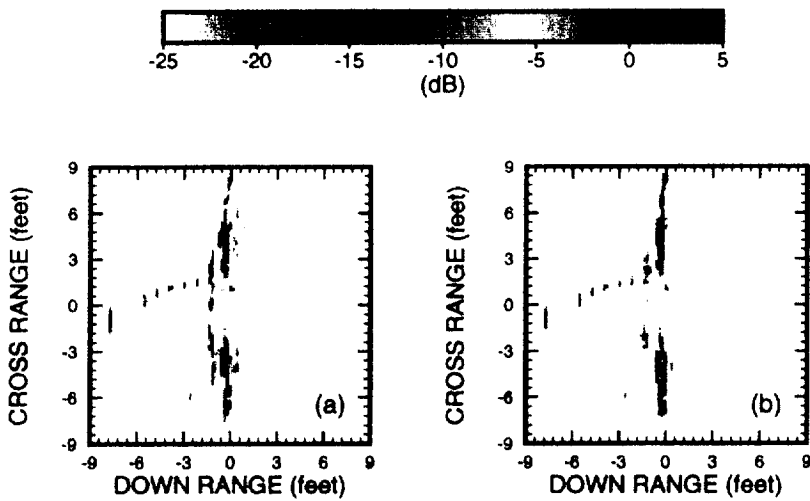
Figure 4.5: Original data (a) and reconstructed data (b) ISAR images of the complex target. 2–6 GHz frequency band and 155° center aspect angle.
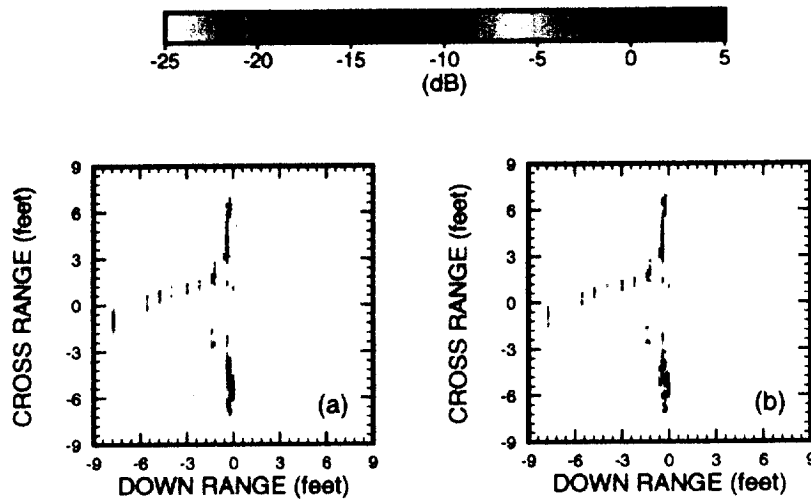
Figure 4.6: Original data (a) and reconstructed data (b) ISAR images of the complex target. 6–12 GHz frequency band and 155° center aspect angle.
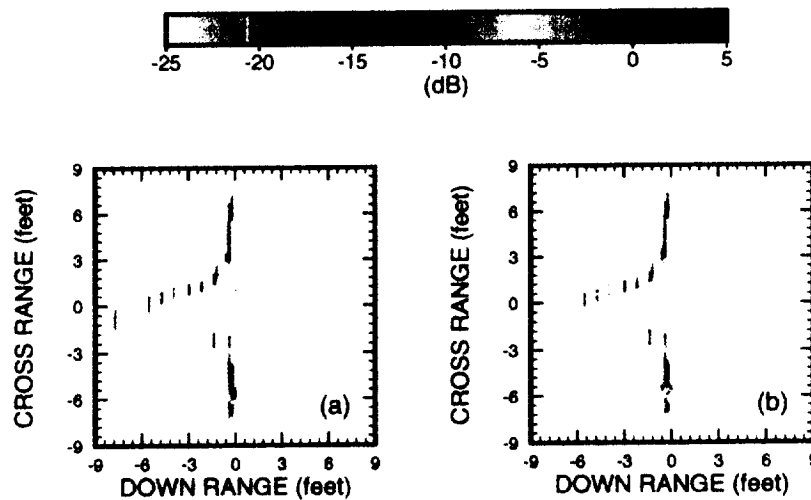

Figure 4.7: Original data (a) and reconstructed data (b) ISAR images of the complex target. 12–18 GHz frequency band and 155° center aspect angle.

19

Table 4.1: Number of line segment and complex point scattering mechanisms detected in three frequency bands.

Frequency Band	2–6 GHz	6–12 GHz	12–18 GHz
Total number of line mechanisms	395	301	448
Minimum number of line mechanisms	0	0	0
Maximum number of line mechanisms	28	33	52
Total number of point mechanisms	2030	1796	1890
Minimum number of point mechanisms	17	17	11
Maximum number of point mechanisms	86	93	121

Correlation between original and reconst. data
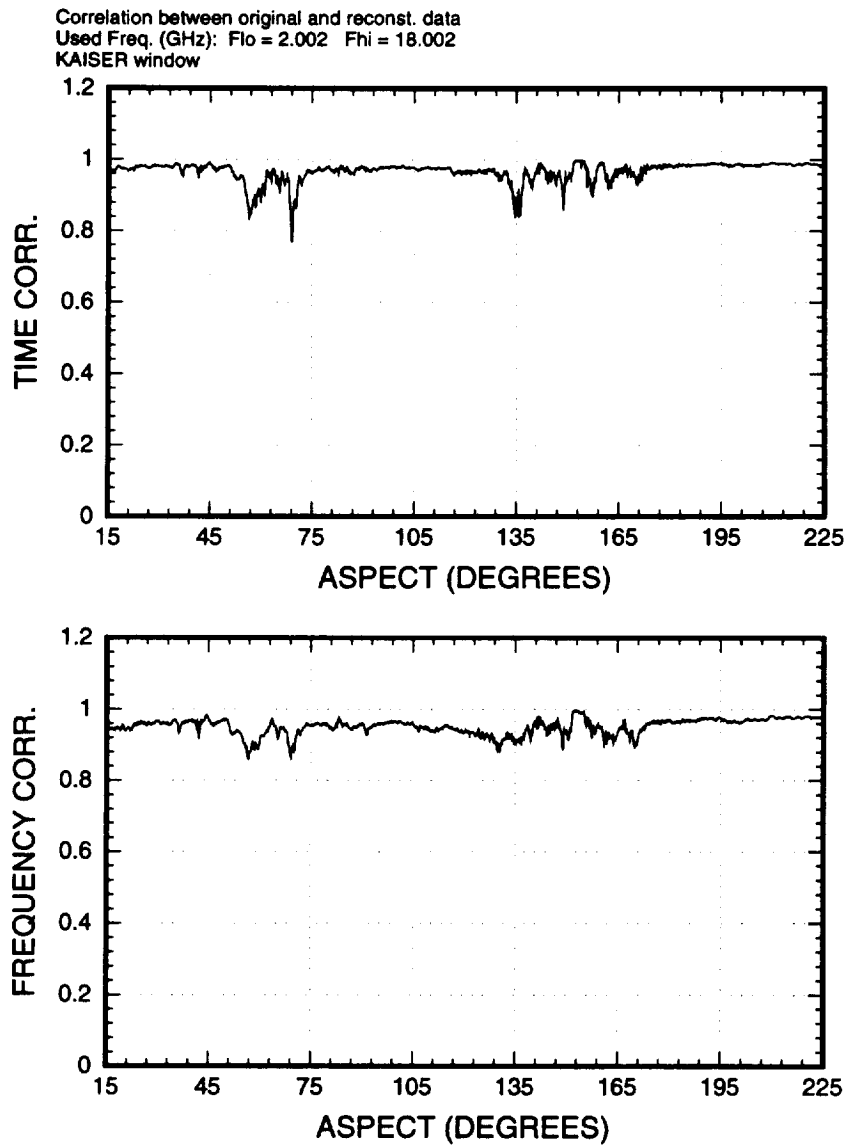Used Freq. (GHz): Flo = 2.002   Fhi = 18.002
KAISER window

Figure 4.8: Time and frequency domain correlation between the original data and the reconstructed data. Maximum number of complex point scattering mechanisms stored is 30.

mechanisms stored for each ISAR image is limited to 30. All other parameters are the same as before. If one compares the plots in this figure with those in Figure 4.1, he/she will find that the correlation between the reconstructed data and the original data is about the same. The total number of complex point mechanism in the three frequency bands, however, is reduced to 1233, 1192 and 1109, respectively. The total size of the compressed data set is now equal to

$$3 \times (5 \times (395 + 1233) + 7 \times (301 + 1192) + 7 \times (448 + 1109)) = 88,470.$$

This leads to a compression ratio of approximately 38, which is excellent.

Figure 4.9–4.11 show the original data ISAR images and the ISAR images obtained using the reconstructed data at 70° center aspect angle. Maximum number of complex point mechanisms used in the reconstructed data is limited to 30. Figure 4.9 contains the ISAR images for 2–6 GHz frequency band. Figure 4.10 contains the ISAR image for 6–12 GHz frequency band, and Figure 4.11 contains the ISAR image for 12–18 GHz frequency band. In all the figures plot (a) is the ISAR image obtained using the original data and plot (b) is the ISAR image obtained using the reconstructed scattered field data. Note that the two images (original data image and the reconstructed data image) look very similar. The main scattering features of the target have been preserved in the reconstructed data image. If one compares these images with the images in Figures 4.2–4.4, he/she will notice that some details are missing in the reconstructed data images in Figures 4.9–4.11. This is because the number of complex point scattering mechanisms used to reconstruct the scattered field data has been limited to 30, and at this aspect angle the radar image of the target is described by many point scattering centers. Nevertheless, the reconstructed data images are a good representation of the original data images.

Figures 4.12–4.15 show the original data images and the reconstructed data images at various center aspect angles. The scattered field data over 6–12 GHz frequency band is used to generate these images. All other parameters are the same as before. Note that for all center aspect angles, the reconstructed scattered field data image shows good agreement with the original scattered field data image in spite of the
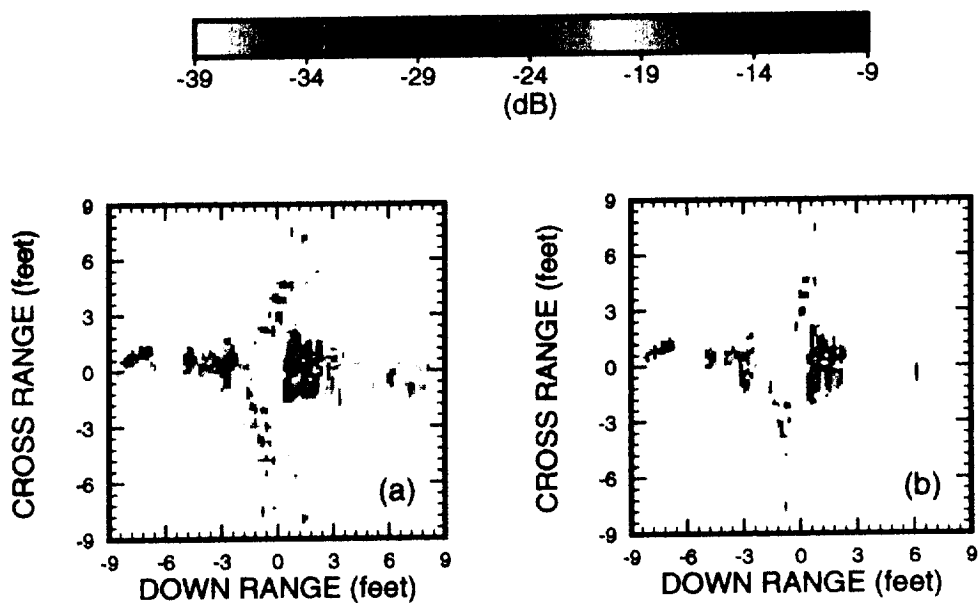
Figure 4.9: Original data (a) and reconstructed data (b) ISAR images of the complex target. 2–6 GHz frequency band and 70° center aspect angle. Maximum number of complex point scattering mechanisms stored is 30.
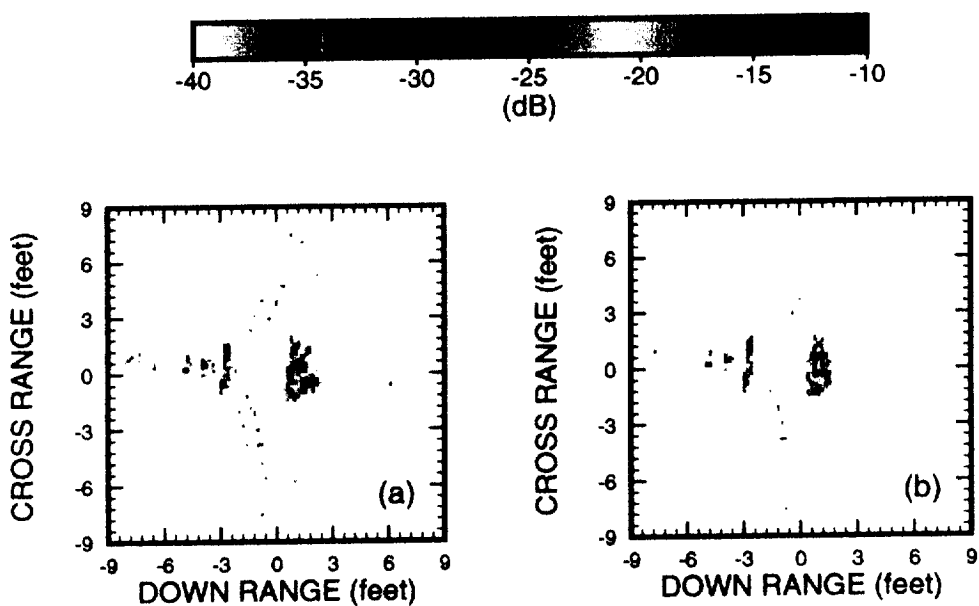

Figure 4.10: Original data (a) and reconstructed data (b) ISAR images of the complex target. 6–12 GHz frequency band and 70° center aspect angle. Maximum number of complex point scattering mechanisms stored is 30.
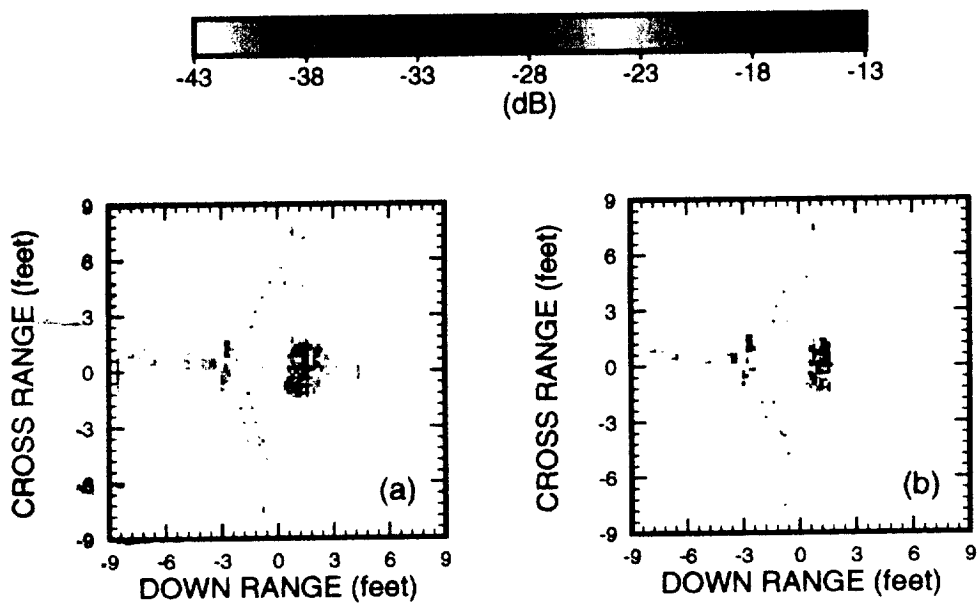
Figure 4.11: Original data (a) and reconstructed data (b) ISAR images of the complex target. 12–18 GHz frequency band and 70° center aspect angle. Maximum number of complex point scattering mechanisms stored is 30.
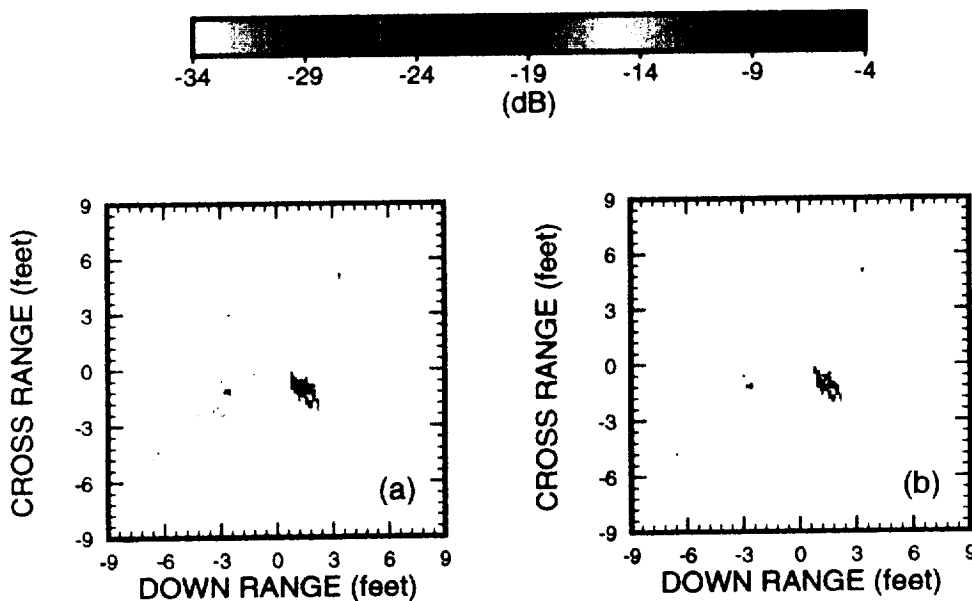

Figure 4.12: Original data (a) and reconstructed data (b) ISAR images of the complex target. 6–12 GHz frequency band and 30° center aspect angle. Maximum number of complex point scattering mechanisms stored is 30.

Figure 4.13: Original data (a) and reconstructed data (b) ISAR images of the complex target. 6–12 GHz frequency band and 110° center aspect angle. Maximum number of complex point scattering mechanisms stored is 30.
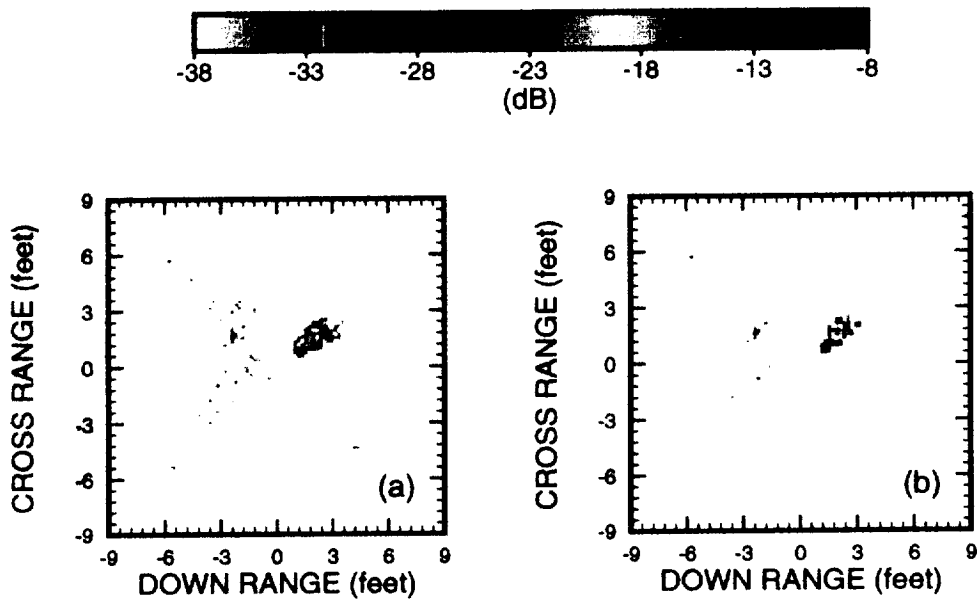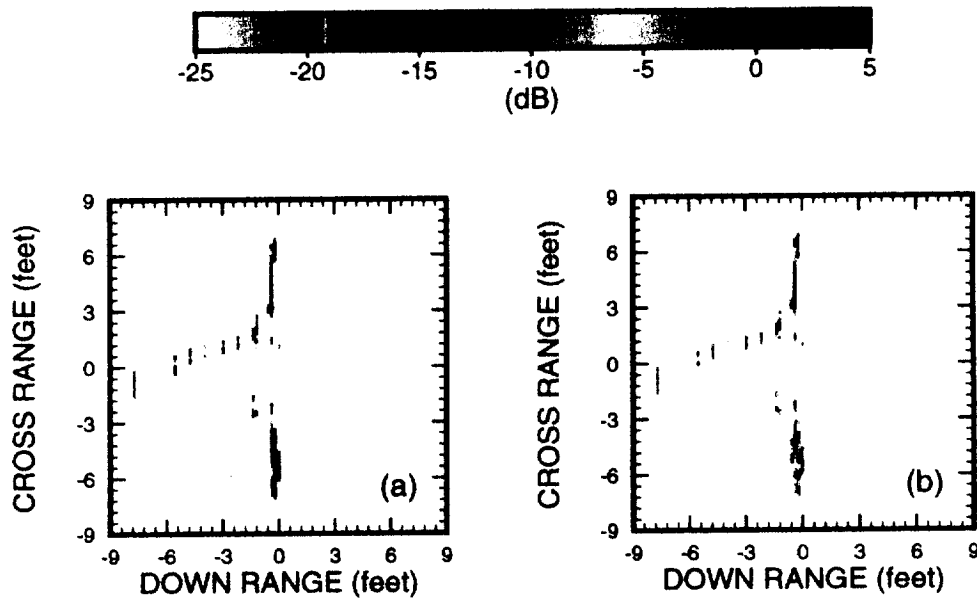

Figure 4.14: Original data (a) and reconstructed data (b) ISAR images of the complex target. 6–12 GHz frequency band and 155° center aspect angle. Maximum number of complex point scattering mechanisms stored is 30.
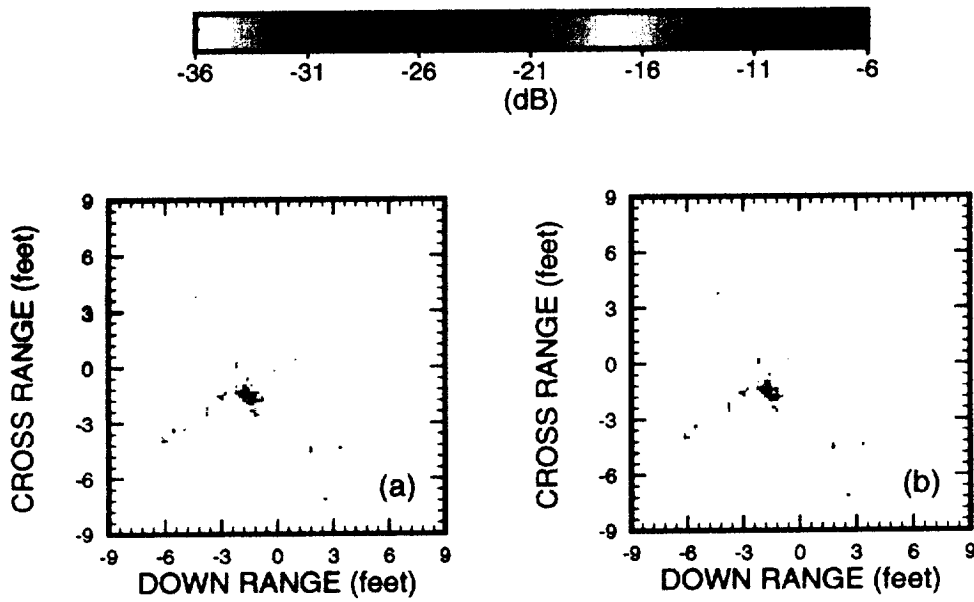
Figure 4.15: Original data (a) and reconstructed data (b) ISAR images of the complex target. 6–12 GHz frequency band and 210° center aspect angle. Maximum number of complex point scattering mechanisms stored is 30.

fact that only 30 point scattering mechanisms are used in the data reconstruction. The main features of the target are preserved. The reconstructed data image in Figure 4.14 shows a remarkable agreement with the original data image. The reason for such a good agreement is that the radar image of the target for 155° center aspect angle is mainly defined by line segment scattering mechanisms. Overall, the data compression technique is quite effective. A summary and general conclusions of this work are given in the next chapter.

Chapter 5

Summary and Conclusions

In this report, a technique is presented to compress the scattered field data from complex targets. The technique is based on the fact that at high frequencies the electromagnetic scattering from complex radar targets exhibit a highly localized behavior. The responses of these localized behavior (scattering mechanisms) are extracted and sampled in the technique. The compression technique preserves the angle as well as frequency variation of individual scattering mechanisms and thus leads to small reconstruction error. The technique uses the focused radar image of a target to estimate the locations of various scattering mechanisms associated with the target. The individual scattering mechanisms, instead of being viewed as isolated scattering centers, are classified into two groups — complex point scattering mechanisms and line segment scattering mechanisms. Different methods are used to sample the two mechanisms.

A complex target can have an extremely large number of scattering mechanisms. If one stores all of these mechanisms, the compression ratio will be poor. To solve this problem, a threshold level is set in the image domain so that the scattering mechanisms whose image magnitude is greater than the threshold level are extracted and stored. As expected, the lower the threshold, the smaller the reconstruction error and the poorer the compression ratio. The technique presented here is designed so that the highest compression ratio and the smallest reconstruction error can be obtained. The technique has been successfully applied to real-world targets. The reconstructed scattered fields of these targets have good correlation with the original

scattered fields. For the example target considered in this report, the compression ratio is as high as 38. Thus, the technique can be used to store the scattered fields for a wide variety of targets without using an astronomical amount of computer storage.

Bibliography

[1] D.J. Andersh, et al., "XPATCH: A high frequency electromagnetic scattering prediction code and environment for complex three dimensional objects," *IEEE Antennas and Propagation Society Magazine*, Vol. 36, pp. 65–69, February 1994.

[2] N. Tseng, "A very efficient RCS data compression and reconstruction technique," M.S. Thesis, Dept. of Elec. Eng., The Ohio State University, Columbus, Ohio, 1992.

[3] Y.S. Oh et al., "Fast line detection algorithm using multivalued image coding," *Electronics Letters*, vol. 26, no. 17, pp. 1400–1402, August 1990.

[4] J. Lee and I. Jurkevich, "Coastline detection and tracing in SAR images," *IEEE Trans. on GeoScience and Remote Sensing*, vol. 28, no. 4, pp. 662–668, July 1990.

[5] L-C. T. Chang, "Removal of undesired scattering centers using a radar image technique," M.S. Thesis, Dept. of Elec. Eng., The Ohio State University, Columbus, Ohio, 1993.